

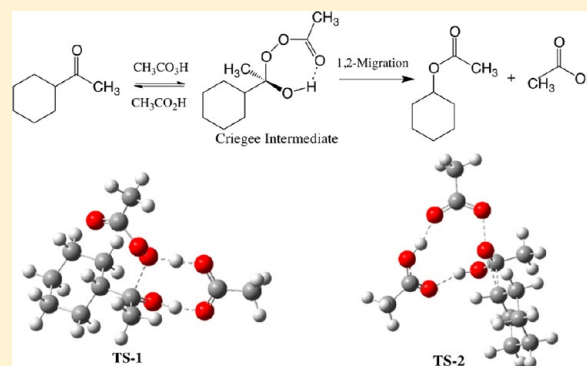
# The Role of Acid Catalysis in the Baeyer–Villiger Reaction. A Theoretical Study

Robert D. Bach\*

Department of Chemistry and Biochemistry, University of Delaware, Newark, Delaware 19716, United States

**S** Supporting Information

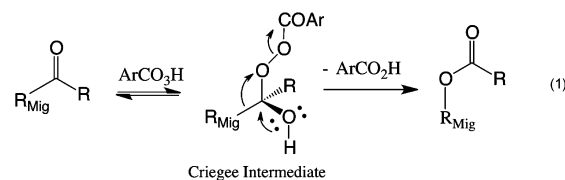
**ABSTRACT:** Quantum mechanical calculations at the B3LYP/6-311+G(d,p) level have examined the overall mechanism of the Baeyer–Villiger (BV) reaction with peroxyacetic acid. A series of reactions that include both the addition step and the subsequent alkyl group migration step included ketones, acetone, *t*-butyl methyl ketone, acetophenone, cyclohexyl methyl ketone, and cyclohexyl phenyl ketone. The combined data suggested that the first step for addition of the peroxyacetic acid oxidation catalyst to the ketone carbonyl to produce the Criegee or tetrahedral intermediate is rate-limiting and has activation barriers that range from 38 to 41 kcal/mol without the aid of a catalyst. The rate of addition is markedly reduced by the catalytic action of a COOH functionality acting as a donor–acceptor group affecting both its proton transfer to the ketone C=O oxygen in concert with transfer of the OOH proton to the carboxylic acid carbonyl. The second or alkyl group migration step has a much reduced activation barrier, and its rate is not markedly influenced by acid catalysis. The rate of both steps in the BV reaction is greatly influenced by the catalytic action of very strong acids.



## INTRODUCTION

The Baeyer–Villiger (BV) reaction remains an important transformation in synthetic organic chemistry because of its unique ability to convert a ketone into an ester or a lactone. This highly useful conversion is readily achieved by using a peroxyacid as the electron-donating reagent that inserts an oxygen atom into a C–C bond adjacent to a carbonyl group ( $C-C=O + O \rightarrow C-O-C=O$ ). This reaction is especially important because it is difficult to achieve this novel change in functionality by other means. The reaction is more effective when the peroxy acid has an electron-withdrawing group such as trifluoroperacetic acid or hydrogen peroxide in conjunction with a Lewis acid. Despite the fact that this oxidative process was first disclosed by Baeyer and Villiger<sup>1</sup> well over 100 years ago and has been studied extensively, there are still aspects of its mechanism that remain controversial as discussed in several reviews.<sup>2</sup> The essential mechanistic fundamentals for this conversion were first described by Criegee more than 60 years ago.<sup>3a</sup> He proposed a two-step process where the peroxyacid first adds to the carbonyl group of the ketone to form a tetrahedral hemiperacetal intermediate (typically referred to as the Criegee intermediate). In the second step, one of the adjacent R groups of the ketone migrates to the proximal oxygen of the perester in concert with O–O bond cleavage and reforms the ketone carbonyl group (eq 1). The primary stereoelectronic effect for the Criegee rearrangement was defined by Kishi<sup>3b</sup> as the bond that is antiperiplanar to the dissociating peroxide bond is always and exclusively the bond that migrates. One of the points of contention is the

mechanism for addition to the carbonyl group and how the hemiperacetal hydrogen migrates to the carboxylate to produce the final products, an ester functionality and a carboxylic acid.



The reaction is particularly useful for the production of lactones, and the regioselectivity of the resulting cyclic ester depends upon the relative migratory ability of the two substituents bound to the ketone. In general, groups that are capable of stabilizing a positive charge appear to migrate preferentially. There is basic agreement that the migratory aptitude decreases in the order *tert*-alkyl > cyclohexyl > *sec*-alkyl > benzyl > phenyl > *primary*-alkyl > cyclopentyl > methyl.<sup>2</sup> However, there is little consensus on why cyclohexyl is so high in this order and phenyl so low.

Whether the first or second step is rate-limiting and if acid catalysis increases the rate of either step is also a matter of controversy. There is not yet agreement on whether acid catalysis involves protonation of the carbonyl oxygen in an ionic stepwise tetrahedral intermediate or if addition to the carbonyl occurs in a concerted neutral manner. Doering<sup>4</sup>

Received: April 9, 2012

Published: July 31, 2012

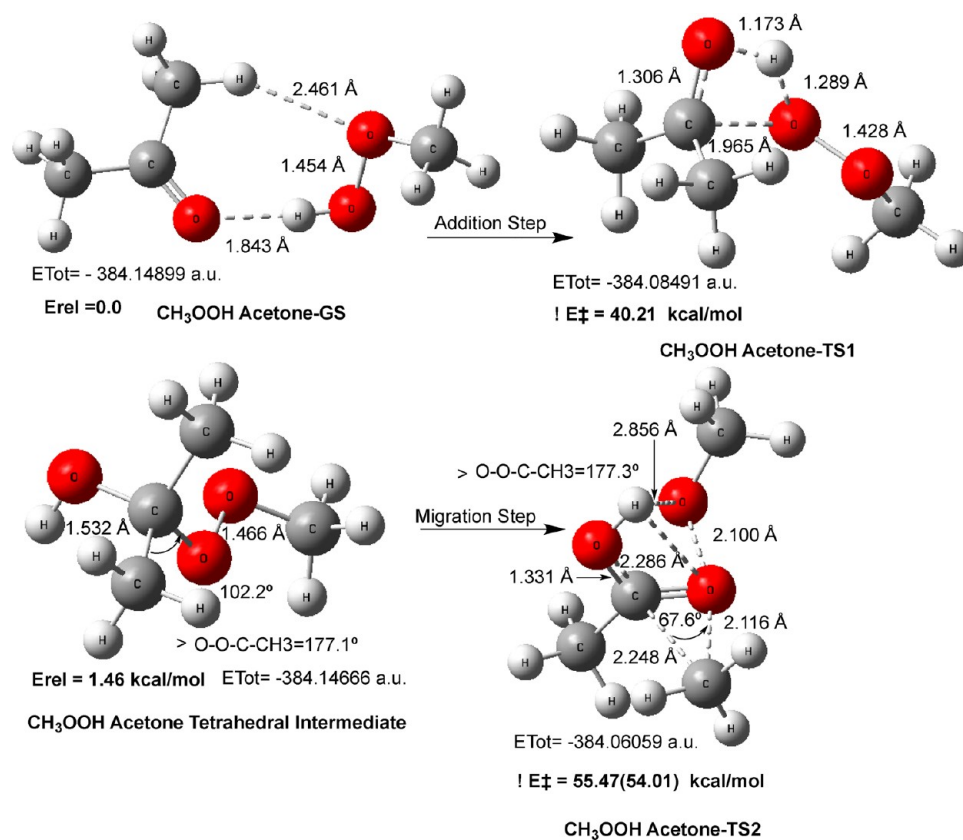


**Figure 1.** Ground-state (GS) complex and first transition state (TS1) for the addition of  $\text{CH}_3\text{OOH}$  to acetone to form the Criegee tetrahedral intermediate and TS2 for the methyl group migration to produce methyl acetate and methanol (eq 2). The barrier in parentheses is calculated relative to the tetrahedral intermediate.

provided an important example that has often been overlooked. He showed that using 13 vol % of concentrated sulfuric acid as solvent for the rearrangement of benzophenone decreased the reaction time to only 30 min as compared to 8 days in acetic acid solvent. Using a highly reactive peroxy acid such as trifluoroperacetic acid (TFPAA) poses additional problems because the byproduct trifluoroacetic acid is a relatively strong carboxylic acid. This can introduce autocatalysis, and the rate-limiting step may also change if the two steps in the BV reaction are influenced differently.

Early studies favored an acid catalyzed rate-limiting migration<sup>5</sup> that was supported by  $^{14}\text{C}$  kinetic isotope effects (KIE) and a negative  $\rho$  value for the Hammett plot of this series of *p*-substituted acetophenones. However,  $^{14}\text{C}$  labeling studies have also been interpreted as evidence for a rate-determining first step involving carbonyl addition depending upon the electron-donating or -withdrawing nature of the ketone involved.<sup>6</sup> More recently, Singleton<sup>7</sup> reported intra- and intermolecular KIE effects for the oxidation of cyclohexanone, suggesting that the first step is rate-determining in the systems studied. Obviously, this overall mechanism still remains a point of controversy, and different reaction conditions can markedly influence the mechanism and the rate-limiting step.

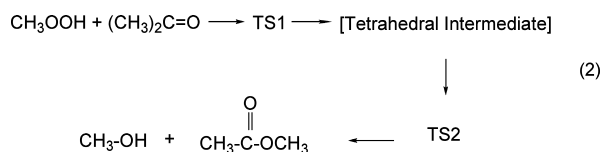
Despite the tremendous amount of experimental work that has been reported for the BV reaction over the years, the extent of high-level theoretical data on the mechanism has been rather limited. To understand how this transformation actually occurs, it is necessary to include the role of Bronsted acid catalysis for both addition (TS1) and migration steps (TS2). In an earlier theoretical study, Okuno<sup>8</sup> suggested that carbonyl addition

corresponds to the rate-determining step and that acid catalysis can contribute to the rate of this step. Theoretical results of Grien et al.<sup>9</sup> also suggest that the first step is rate-determining even in the presence of an acid catalyst. A significant point made was that, while the introduction of an acid catalyst can lead to a reduction in activation energy for the addition step (first TS), if entropy effects are included any gain in enthalpy is typically lost. This observation is particularly relevant because a subsequent study by Yamabe<sup>10</sup> stressed the importance of hydrogen bonding in the addition step and proposed that BV reactions occur via a complex involving a ketone and a trimer of three molecules of peracid (peroxyformic acid). This hypothesis was immediately challenged by Alvarez-Idaboy and colleagues<sup>11</sup> in a series of papers that thoroughly discussed the problems associated with using the calculated total energies as the zero or reference point to measure activation barriers rather than free energies. It was demonstrated<sup>11b</sup> that the total  $\Delta G$  involved in the process of trimer formation was positive (7.36 kcal/mol), and consequently with the proper zero point the calculated barrier for the addition (step one) to acetone would be increased from 24.75 to 32.35 kcal/mol, a prohibitive barrier! They also presented a new mechanism for the addition of peroxyacetic acid to acetone that involved a molecule of acetic acid acting as an acid catalyst. In the TS, the acetic acid transfers its proton to the ketone oxygen in concert with the peroxyacid proton being transferred to the acetic acid carbonyl oxygen. The free energy barrier for this addition step (TS1) was 12.7 kcal/mol lower than any TS previously reported. In the present study, we expand upon this novel observation and provide explanations in support of the origin of the observed

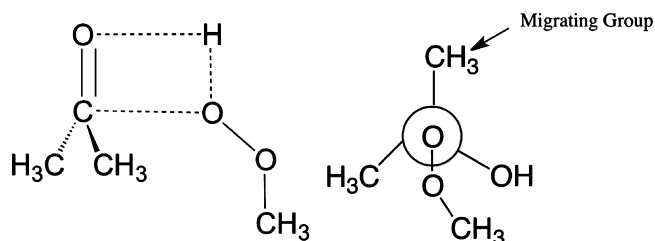
migratory aptitude for the series of ketone substituents noted above. There have also been several other theoretical studies on this very fundamental reaction that include such topics as  $\text{BF}_3$  catalysis,<sup>12a</sup>  $\alpha\text{-CF}_3$  directing effects,<sup>12b</sup> anti versus gauche migratory aptitudes,<sup>12c</sup>  $\text{H}_2\text{O}_2$  catalysis,<sup>12d</sup> and regioselectivity in 3-keto steroids.<sup>12e</sup>

## RESULTS AND DISCUSSION

**a. Methyl Hydroperoxide and Acetone.** Despite the various controversies concerning the mechanism of the BV reaction, it is universally accepted that it involves the formation of a tetrahedral intermediate, the Criegee intermediate. We choose initially to examine the simplest possible peroxide and ketone that could arrive at the tetrahedral intermediate (eq 2). If this is truly a neutral concerted process, then the transition state (TS) proceeds via a four-member ring with the O–H adding across the ketone  $\text{C}=\text{O}$ . Such a cyclic TS has four frontier orbital electrons, and consequently it would be disfavored based upon orbital symmetry considerations.<sup>13</sup> Although one can assume that the HOMO and LUMO will have different orbital symmetries, the TS is not rigorously cyclic in terms of the orbital overlaps so the net overlap is not necessarily zero. The interaction of methyl hydroperoxide with acetone is shown in Figure 1. Examination of TS1 shows that the O–H bond ( $r_{\text{OH}} = 1.173 \text{ \AA}$ ) forms well ahead of C–O bond making ( $r_{\text{C-O}} = 1.965 \text{ \AA}$ ). As anticipated, the classical activation barrier ( $\Delta E^\ddagger$ ) of 40.21 kcal/mol is consistent with what could be termed as an antiaromatic or formally forbidden reaction and is far in excess of that for a reaction that proceeds readily. The very high single imaginary frequency for TS1 ( $\nu_i = 1531.4i \text{ cm}^{-1}$ ) is indicative of a TS with major involvement of light atom (hydrogen) motion. However, the reaction vector does contain a significant requisite contribution for C–O bond formation.<sup>14a</sup> It is typical for the total energy of the tetrahedral intermediate involved in the BV reaction to be comparable in magnitude to that of the starting ground state (GS) complex, and this is true for this model reaction ( $\Delta E = 1.46 \text{ kcal/mol}$ ). The TS for the migration step (TS2) in Figure 1 also exhibits a very high classical barrier ( $\Delta E^\ddagger = 55.47 \text{ kcal/mol}$ ). It is quite easy to identify the concerted 1,2-migration induced by the O–O bond breaking and attendant C–C bond elongation (2.248  $\text{\AA}$ ) of the  $\text{CH}_3$  group. The migrating group is always antiperiplanar to the migration terminus as evidenced by the above Newman projection where the O–O–C–CH dihedral angle is  $177.3^\circ$ . The high barrier is also a direct consequence of the highly elongated O–O bond (2.100  $\text{\AA}$ ). The absence of the stabilizing influence of the  $\text{C}=\text{O}$  group present in a peroxy acid also contributes to this high barrier. It has generally been assumed that a negatively charged oxygen on the tetrahedral intermediate would rearrange faster. However, in TS2 there is little opportunity for the OH group on this Criegee intermediate to dissociate to provide such a negative charge, and consequently we see a very high migration barrier.



The important discovery by Alvarez-Idaboy<sup>11</sup> that a carboxylic acid group could act as a catalyst for the addition step of a peroxy acid to the  $\text{C}=\text{O}$  group in the BV reaction



prompted us to examine this possibly for our model reaction. Acetic acid has both a hydrogen donor and acceptor in the same molecule as evidenced by the fact that it readily forms very stable dimers, and consequently its boiling point is atypically high. The ground-state prereaction complex (Figure 2) for peroxyacetic acid, acetone, and acetic acid (HOAc) demonstrates the electropositive nature of the OH group and the electronegativity of its carbonyl oxygen as it H-bonds to the OOH group of the peroxy acid. The calculated stabilization energy for this GS complex is relatively large ( $\Delta E = -23.61 \text{ kcal/mol}$ ), while its free energy is slightly positive ( $\Delta G = 0.51 \text{ kcal/mol}$ ), reflecting the negative entropy for bringing the three reactants together as so adroitly described by Alvarez-Idaboy et al.<sup>11b</sup> Nonetheless, we will still present the classical activation barriers based upon total energies because it is the relative barriers that we stress in this Article. We do provide free energies of activation for selected more relevant examples, and the data are available in the Supporting Information to calculate free energies of activation.

The classical activation barrier ( $\Delta E^\ddagger = 16.09 \text{ kcal/mol}$ ) for the addition of  $\text{CH}_3\text{OOH}$  to acetone was markedly lowered by the catalytic action of HOAc. The single imaginary frequency for this TS was ( $\nu_i = 550.3i \text{ cm}^{-1}$ ) indicative<sup>14a</sup> of both hydrogen and heavy atom motion as the OH and carbonyl carbon move toward each other to form the C–O bond of the tetrahedral intermediate. The requirement for  $\text{CH}_3\text{OOH}$  addition to the  $\text{C}=\text{O}$  with a relatively low barrier is transfer of its OOH proton to the HOAc carbonyl oxygen in concert with proton transfer from HOAc to the ketone carbonyl oxygen to make it more receptive to nucleophilic addition. The tetrahedral intermediate product was 0.51 kcal/mol higher in energy than the GS, but its free energy is 6.05 kcal/mol greater. The barrier for the  $\text{CH}_3$  migration, while considerably lower than that without catalysis, is still quite high with TS2 having  $\Delta E^\ddagger = 32.98 \text{ kcal/mol}$ . The C–O and O–O bond elongations are 1.823 and 1.929  $\text{\AA}$  with the HOAc exhibiting both donor and acceptor interactions.

**b. Peroxyacetic Acid and Acetone.** By increasing the complexity of the oxidizing agent from methyl hydroperoxide to peroxyacetic acid, we include an additional  $\text{C}=\text{O}$  functional group. In preliminary calculations, we used peroxyformic acid and found that the concerted four-membered TS for addition to acetone also exhibited a very high barrier ( $\Delta E^\ddagger = 39.56 \text{ kcal/mol}$ ), but TS2, the migration step, had a barrier that was much reduced from that observed above for  $\text{CH}_3\text{OOH}$  ( $\Delta E^\ddagger = 23.49 \text{ kcal/mol}$ ). These structures are given in the Supporting Information (Figure S1). That we may make a more direct comparison with the corresponding data reported by Alvarez-Idaboy,<sup>11a</sup> we have concentrated upon similar TSs derived from peroxyacetic acid. The addition step for peroxyacetic acid to acetone proceeds, as expected, in a fashion similar to that noted for peroxyformic acid and also had a very high activation barrier ( $\Delta E^\ddagger = 37.86 \text{ kcal/mol}$ ) for the uncatalyzed addition (Figure 3). In PAA-TS1, the O–O bond remains essentially intact,

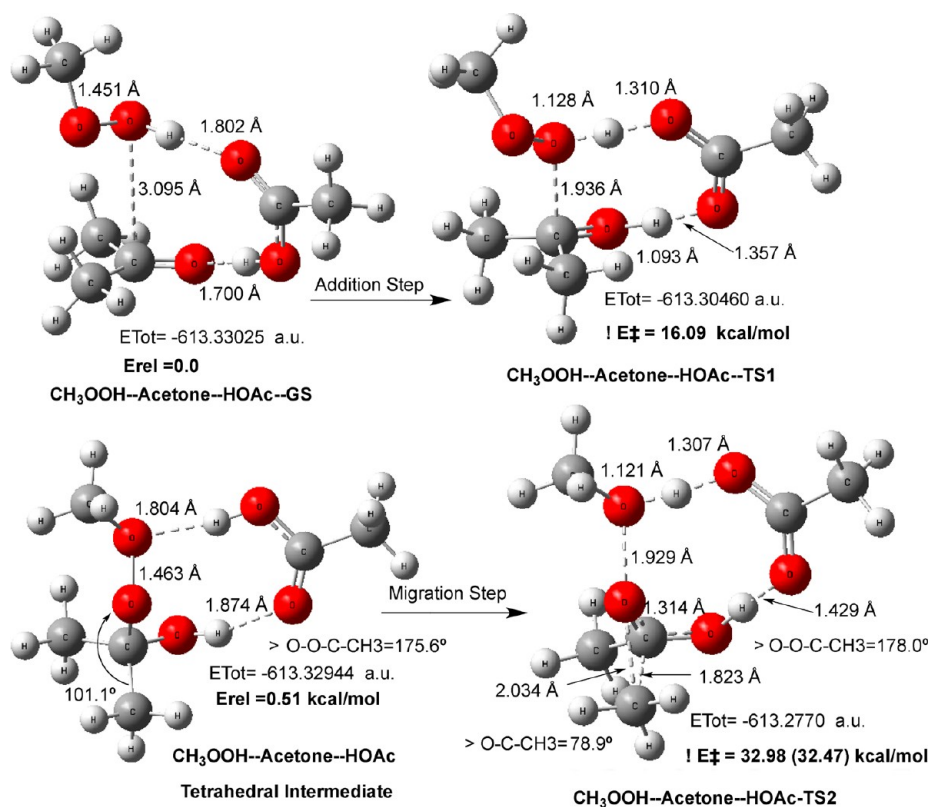


**Figure 2.** Ground-state (GS) complex including acetic acid (HOAc) as a catalyst and the first transition state (TS1) for the addition of CH<sub>3</sub>OOH to form the Criegee tetrahedral intermediate. The transition state (TS2) for methyl group migration produces methyl acetate and methanol (eq 1). The barrier in parentheses is calculated relative to the tetrahedral intermediate.

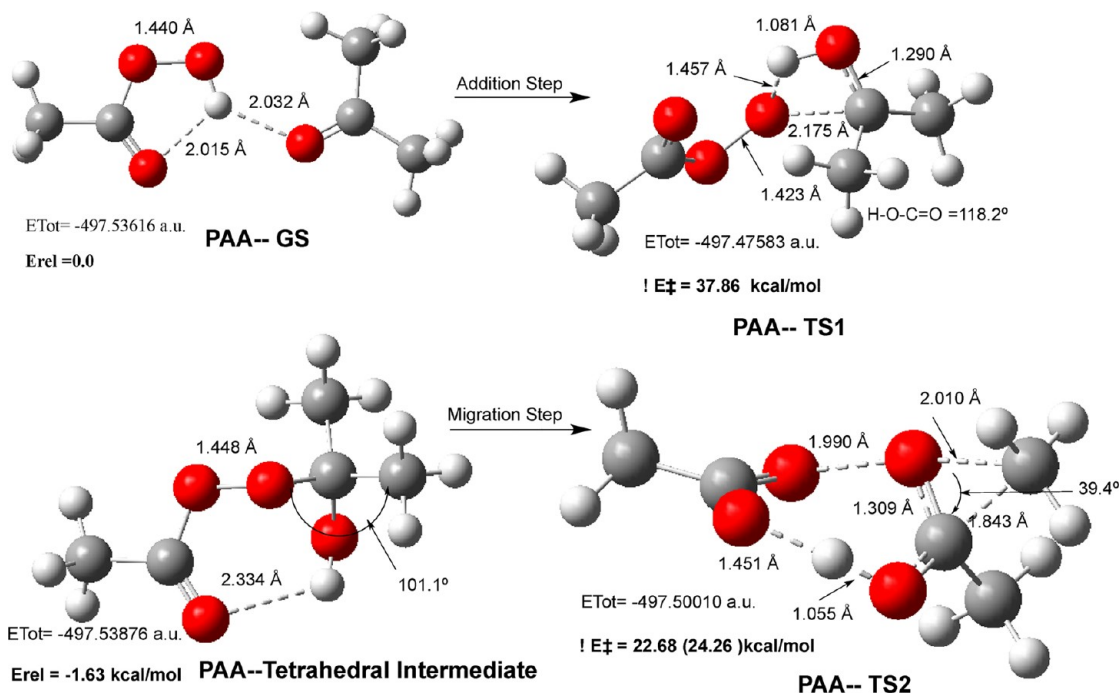
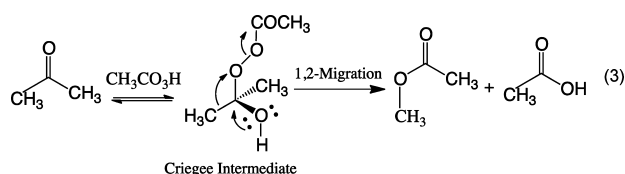


**Figure 3.** Ground-state (GS) complex and the first transition state (TS1) for the addition of CH<sub>3</sub>CO<sub>3</sub>H to acetone to form the Criegee tetrahedral intermediate. The transition state (TS2) for the methyl group migration produces methyl acetate and acetic acid.

while the developing O–C bond (2.175 Å) is still quite elongated. The O–H bond of the peroxy acid is largely transferred to the ketone carbonyl oxygen in the cyclic TS ( $r_{\text{O-H}} = 1.081$  Å). As noted above for the peroxyformic acid

migration step, the barrier for TS2 is comparable and is also markedly reduced ( $\Delta E^\ddagger = 22.68$  kcal/mol). The C=O group of the peroxy acid accepts the proton from the tetrahedral intermediate OH group to allow for migration of the CH<sub>3</sub>

group in TS2, thereby lowering the barrier. The barrier in parentheses is calculated relative to the tetrahedral intermediate. While calculation of TS2 from the reactant or GS complex is perhaps kinetically more correct because the mechanism for the Criegee intermediate applies the steady-state approximation, from a mechanistic perspective it is also nice to know the barrier relative to the discrete tetrahedral intermediate formed in this reaction. In each figure, we include the barriers relative to the GS complex, the relative energy of the Criegee intermediate, and the activation barrier relative to this intermediate (in parentheses).



When acetic acid is included as an acceptor–donor catalyst, the activation barriers drop significantly as first reported by Alvarez-Idaboy.<sup>11a</sup> The free energy for formation of the ground-state complex (PAA–HOAc–GS) is essentially zero ( $\Delta G = 0.024$  kcal/mol) as a consequence of entropy effects. However, the calculated stabilization energy was  $-22.62$  kcal/mol based

upon total energies reflecting the series of relatively strong H-bonds that hold this prereaction complex together. The reactants are held in the proper juxtaposition for the distal oxygen of the OOH bond to add to the carbonyl carbon ( $r_{O-C} = 2.986$  Å, Figure 4) of the ketone with a classical barrier of 18.83 kcal/mol and a free energy of activation  $\Delta G^\ddagger = 19.80$  kcal/mol. It is noteworthy that this addition no longer involves a four-membered ring TS because instead of the OH group adding across the C=O in a cycloaddition fashion, its hydrogen is transferred to the HOAc carbonyl oxygen. Consequently, we observe the activation barrier to be only about one-half of that of the corresponding addition step in the absence of the acetic acid catalyst ( $\Delta\Delta G^\ddagger = 19$ ). The reduction in the barrier for step one (12.7 kcal/mol) for this same reaction reported by Alvarez-Idaboy<sup>11a</sup> was based upon free energies of activation relative to isolated reactants and included a SCI-PCM solvent correction.

The relatively large imaginary frequency for TS1 (Figure 4, PAA–HOAc–TS) ( $\nu_i = 811.7i$  cm<sup>-1</sup>) is consistent with mostly light atom motion. Animation of the reaction vectors demonstrates nearly complete proton transfer to the ketone carbonyl in concert with hydrogen transfer from the OOH group to the HOAc carbonyl oxygen oscillating back and forth in a ping-pong fashion. The reaction vectors for C–O bond

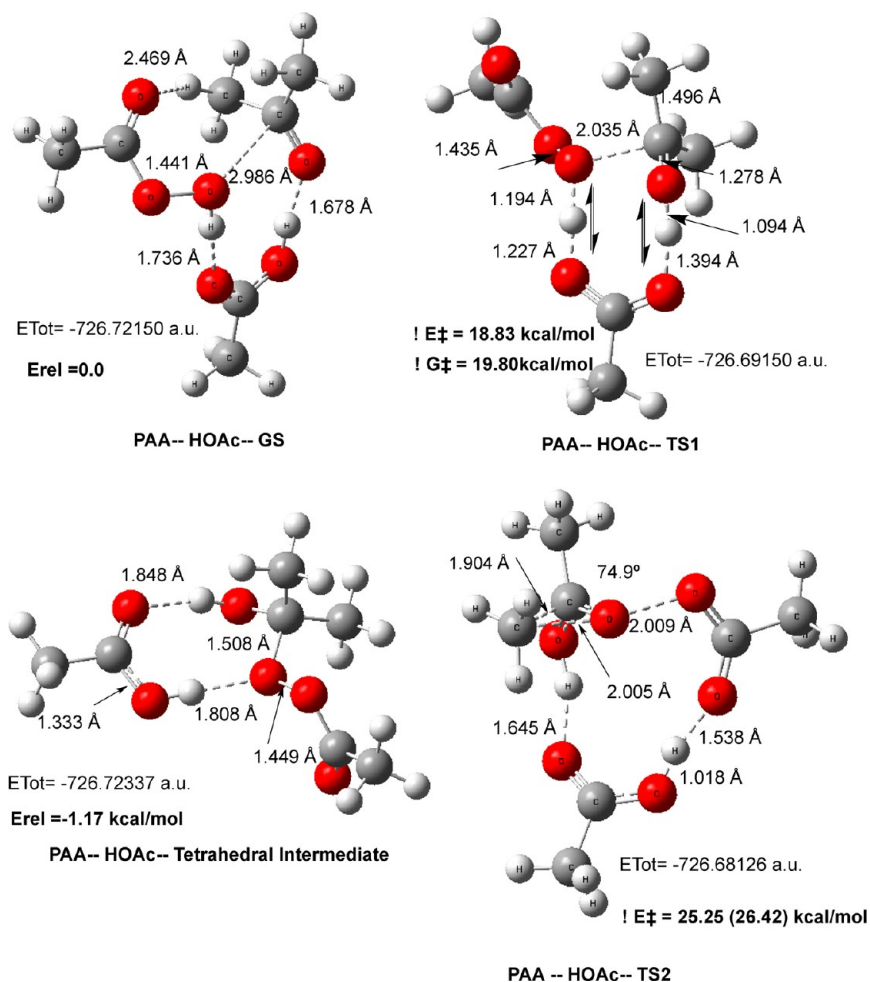


**Figure 4.** Ground-state (GS) complex for peroxyacetic acid and acetone with acetic acid (HOAc) catalysis and the first transition state (TS1) for the addition of  $\text{CH}_3\text{CO}_3\text{H}$  to acetone to form the Criegee tetrahedral intermediate. The transition state (TS2) for the methyl group migration produces methyl acetate and acetic acid.

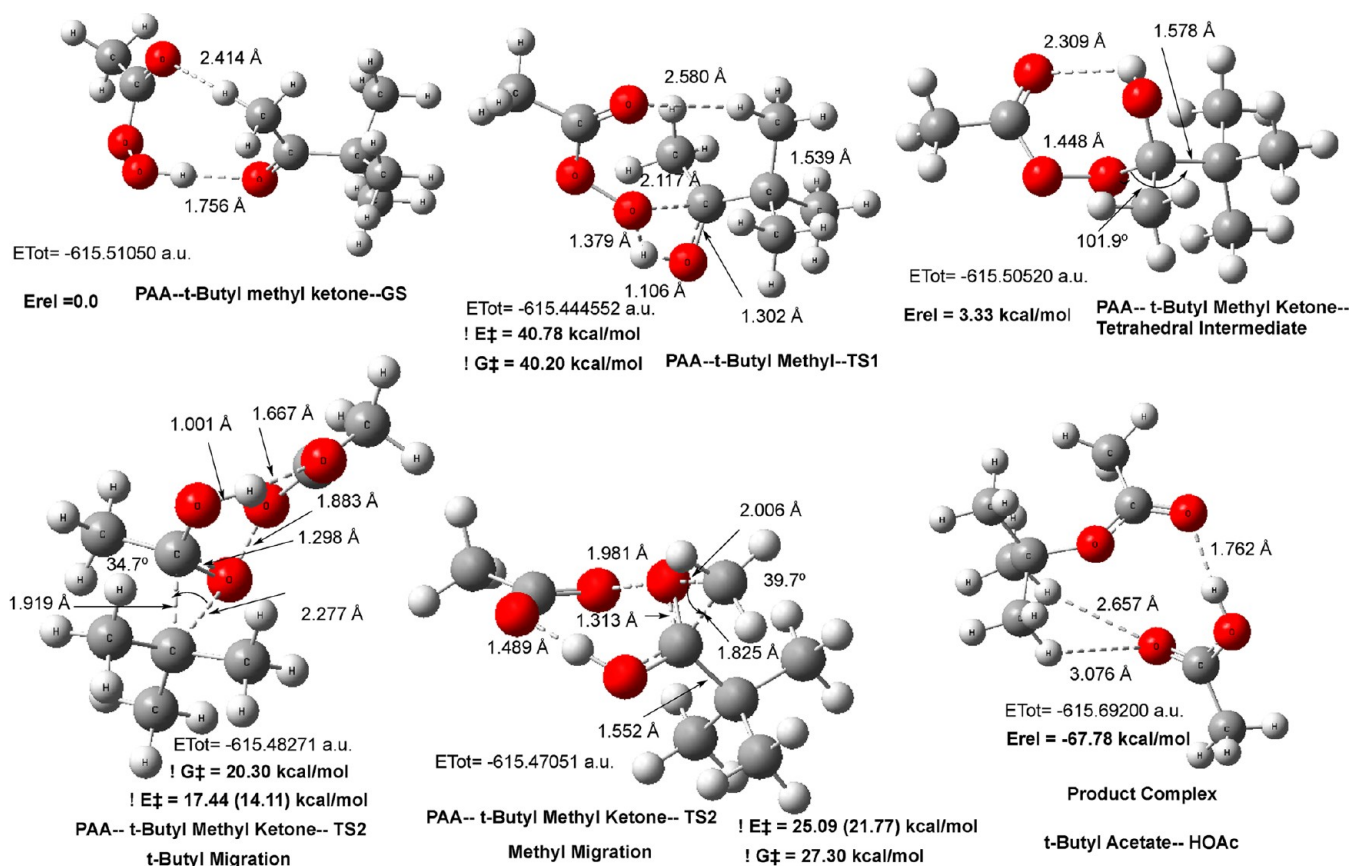


**Figure 5.** Ground-state (GS) complex for peroxyacetic acid and *t*-butyl methyl ketone and the first transition state (TS1) for the addition of  $\text{CH}_3\text{CO}_3\text{H}$  to form the Criegee tetrahedral intermediate. The transition state (TS2) for the *t*-butyl group migration produces *t*-butyl acetate and acetic acid.

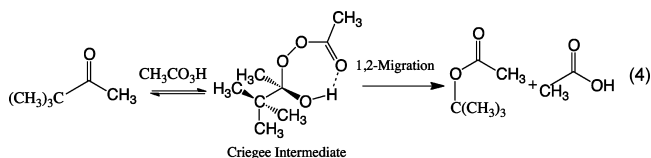
formation (0.45) and each of the two proton transfers (0.41) are nearly comparable in magnitude. In this instance, the tetrahedral intermediate is slightly lower in energy ( $\Delta E = -1.17$  kcal/mol), and the activation barrier ( $\Delta E^\ddagger = 25.25$  kcal/mol) for the second rearrangement step, TS2, relative to the total energy of the tetrahedral intermediate is also lower than TS1. A proton relay is involved as the tetrahedral intermediate OH proton is transferred to the HOAc catalyst, and it transfers its proton to the departing acetate moiety that has an O–O bond elongation of 2.009 Å. Methyl group migration is induced by a developing negative charge on the leaving acetate moiety. An NBO analysis suggests that the negative charges on the  $\text{O}(\text{C}=\text{O})\text{CH}_3$  fragment for the GS, TS1, the tetrahedral intermediate, and TS2 are  $-0.081$ ,  $-0.070$ ,  $-0.572$ , and  $-0.492e$ . This charge must be complimented by a corresponding positive charge on the developing ester group that effects alkyl group migration. This barrier is in good agreement with that reported by Alvarez-Idaboy.<sup>11a</sup> The extent of O–O and C–C bond breaking is lessened and largely responsible for the reduction in barrier relative to the uncatalyzed migration step.

We have been encouraged to compare our results with those that use more recent DFT functionals (see Computational Details) such as the MPWB1K method used by Alvarez-Idaboy<sup>11a</sup> that has been more specifically developed to treat thermochemical kinetics. The transition structures for the acetone TSs shown above (Figure 4) were quite close for TS1 ( $\Delta\Delta E^\ddagger = 0.63$  kcal/mol), while the barrier for TS involving O–O bond breaking was somewhat higher ( $\Delta\Delta E^\ddagger = 5.73$  kcal/mol). When we employed the MO6-2X functional, the

transition structure for the addition step (TS1) closely resembled that derived from the time tested B3LYP method, and the classical activation barrier ( $\Delta E^\ddagger = 16.39$  kcal/mol) was slightly lower in magnitude ( $\Delta\Delta E^\ddagger = -2.44$  kcal/mol). However, the barrier for the migration step (TS2) where the O–O bond is essentially broken ( $r_{\text{O}-\text{O}} = 1.920$  Å) gave a much higher barrier ( $\Delta\Delta E^\ddagger = 9.75$  kcal/mol) that was clearly out of range for the other TSs that we have examined. In previous reports,<sup>14</sup> we have found that for oxygen transfer the B3LYP functional gives closer agreement with QCISD(T) and CCSD(T) calculations than related functionals as discussed in more detail in the Computational Details.

**c. Peroxyacetic Acid and *t*-Butyl Methyl Ketone.** The substituents that are at both ends of the spectrum of migratory aptitudes in the BV reaction are a tertiary alkyl and a methyl group. Consequently, we have examined the relative activation barriers for alkyl migration in *t*-butyl methyl ketone (eq 4) in an effort to discern some of the factors responsible for this reactivity trend. First, we determine the intrinsic intramolecular competitive migratory barriers in the absence of a catalyst. The requisite prereaction complex is given in Figure 5, and the primary H-bonding interaction is between the OOH group of peroxyacetic acid and the ketone carbonyl oxygen ( $r_{\text{O}-\text{H}} = 1.765$  Å). The unsymmetrical four-center TS has a leading O–H bond (1.106 Å) and a rather long O–C distance (2.117 Å) resulting in a very high TS1 barrier ( $\Delta E^\ddagger = 40.78$  kcal/mol) to afford a tetrahedral intermediate that is 3.33 kcal/mol higher in energy than its GS precursor. For the second step (TS2), hydrogen migration is between the OOH group of peroxyacetic

acid and the ketone carbonyl oxygen ( $r_{\text{O-H}} = 1.765 \text{ \AA}$ ). For the second step (TS2), the migratory barriers for *t*-butyl versus methyl within the same internally consistent molecule are particularly informative. The barrier for *t*-butyl group migration ( $\Delta E^\ddagger = 17.44 \text{ kcal/mol}$ ) is 7.65 kcal/mol lower than that for methyl group migration. However, the relative barriers are further complicated by the fact that the tetrahedral intermediate with the *t*-butyl group antiperiplanar is 5.27 kcal/mol lower in energy than the conformer with the methyl group anti. The actual barrier for  $\text{CH}_3$  group migration relative to this higher energy conformer is 16.50 kcal/mol but is 21.77 kcal/mol relative to the lower energy tetrahedral intermediate. Examination of the two TSs (Figure 5) shows no discernible major differences in steric interactions, and in fact the C–C distance for the *t*-butyl TS is actually longer (1.919 vs 1.825  $\text{\AA}$ ). Conventional wisdom dictates that it is the electron-donating ability of the migrating group that determines its efficacy, and this would seem to be the case. A free energy difference of 7.00 kcal/mol corresponds to a rate difference of more than  $10^4$ , and this is in consonance with observed relative rates.<sup>15a</sup> The overall exothermicity of the BV reaction is also a driving force in its capacity to convert ketones to esters, and this case is no exception with a calculated reaction energy  $\Delta E = -67.78 \text{ kcal/mol}$  (Figure 5).



When acetic acid is included, the ground-state prereaction complex has the ketone carbonyl H-bonded to the HOAc acidic hydrogen as noted previously (Figure 6). Although the reactants are poised in the proper orientation for OOH addition, the O–C distance in the GS complex is 3.143  $\text{\AA}$ , while that in TS1 is reduced to 2.090  $\text{\AA}$ . We again see a marked reduction in activation barrier ( $\Delta E^\ddagger = 20.17 \text{ kcal/mol}$ ) for this HOAc-assisted addition step relative to the uncatalyzed addition ( $\Delta\Delta E^\ddagger = 20.62 \text{ kcal/mol}$ ). The single imaginary frequency ( $\nu_i = 761.7i \text{ cm}^{-1}$ ) reflects the light atom motion evidenced by the H–O hydrogen-bonding distances of 1.238 and 1.186  $\text{\AA}$  for the hydrogen atom oscillating between the distal peroxide oxygen and the acid carbonyl oxygen. The migration step actually has a slightly higher barrier for *t*-butyl migration ( $\Delta E^\ddagger = 18.30 \text{ kcal/mol}$ ) relative to the uncatalyzed TS ( $\Delta\Delta E^\ddagger = 0.86 \text{ kcal/mol}$ ).

We also examined this BV reaction using the MPWB1K functional and found that TS1 was nearly identical to the above B3LYP TS ( $\Delta E^\ddagger = 19.74 \text{ kcal/mol}$ ); however, we were unable to locate TS2 with this functional even when we started with the B3LYP optimized geometry and did a CALCFC to get the correct force constants. The TS structure simply collapsed back to the tetrahedral intermediate. For this reason and those given above, we have continued to use the B3LYP functional when oxygen atom transfer is involved.

**d. Relative Rates of Addition and Migratory Aptitude for Three Methyl-Substituted Ketones.** As noted above, a methyl group is the slowest alkyl group to migrate in the second step of the BV reaction. The better migratory aptitude of a cyclohexyl group versus that of a phenyl group is another question that remains unresolved. This is especially troublesome because it is generally thought that an aryl group at the

carbonyl carbon has a rate-retarding influence on the addition step (TS1). A series of kinetic experiments more than 60 years ago<sup>15a</sup> on several ketones having this requisite substitution pattern now provides us with an opportunity to calculate both reaction steps independently in hopes of resolving these mechanistic issues. The rate constants for the perbenzoic acid oxidation of acetophenone and cyclohexyl phenyl ketone in chloroform solution were shown to be comparable in magnitude, while cyclohexyl methyl ketone was found to be about 6–8 times more reactive over an 8-day reaction period. This led to the suggestion that conjugation of the carbonyl group with an aromatic substituent significantly reduces the reactivity of the ketone toward BV oxidation. However, examination of the free energies derived from the rate constants (Scheme 1) shows that these oxidations are actually relatively slow and that the activation barriers differ by only a little more than a kcal/mol. The free energies of activation based upon our DFT calculations (in parentheses) show a comparable difference. Product distribution studies on cyclohexyl phenyl ketone(III) showed that for the second step in the BV oxidation, the cyclohexyl group migrated about 5 times faster than the phenyl group.<sup>15a</sup> While this kinetic study suggested that the addition step (TS1) was rate-limiting in the presumed absence of a catalyst, a second kinetic study that used TFPAA with trifluoroacetic acid catalysis suggested that the rate-limiting step had now switched from addition to the migration step (TS2).<sup>15b</sup> Evidence was presented that the ketone carbonyl oxygen was protonated by the stronger carboxylic acid.

**1. Acetophenone.** The GS prereaction complex for peroxyacetic acid and acetophenone (I) is shown in Figure 7. The addition step proceeds through a cyclic four-membered TS. The approach of the peroxy acid OH group to the C=O is unsymmetrical with a C–O bonding distance of 2.200  $\text{\AA}$ , and the TS exhibits about the same high barrier as noted above ( $\Delta E^\ddagger = 40.60 \text{ kcal/mol}$ ). The tetrahedral intermediate with the phenyl group anti is somewhat higher in energy than the GS complex ( $\Delta E = 4.76 \text{ kcal/mol}$ ), but the Criegee intermediate with the methyl group anti to the O–O bond is actually a little more stable ( $\Delta E = 0.22 \text{ kcal/mol}$ ). The barrier for phenyl migration in PAA-acetophenone-TS2 is markedly lower than TS1 ( $\Delta E^\ddagger = 22.30 \text{ kcal/mol}$ ) relative to the total energy of the intermediate corresponding to the TS with its phenyl group anti. A distinguishing feature of this migration TS is its relatively short C–Ph distance of only 1.660  $\text{\AA}$ , reflecting the bridging nature of a typical 1,2-phenyl migration. The departing acetic acid moiety is assisted by an H-bonding interaction with the OH group as the O–O bond elongates ( $r_{\text{O-O}} = 1.997 \text{ \AA}$ ) in the TS. An earlier theoretical analysis<sup>15b</sup> of bond orders in the migration step with *m*-chloroperbenzoic acid also suggested that the rearrangement process is a concerted asynchronous transposition where O–O bond breaking is more advanced than aryl migration. It was also noted that a change from an electron-withdrawing *para* substituent to a *para*-methoxy group resulted in a shift in the rate-determining step from aryl migration to the carbonyl addition step.

The barrier for the addition of peroxyacetic acid to acetophenone with HOAc catalysis, PAA-acetophenone-TS1, is again reduced by more than one-half ( $\Delta E^\ddagger = 18.03 \text{ kcal/mol}$ ) as a consequence of negating the four-membered nature of the TS (Figure 8). The TS for phenyl migration is calculated to be 4.50 kcal/mol lower than methyl migration. The rearrangement barrier for TS2 is somewhat lower ( $\Delta\Delta E^\ddagger = 3.28 \text{ kcal/mol}$ ) than the uncatalyzed barrier, reinforcing the generally held

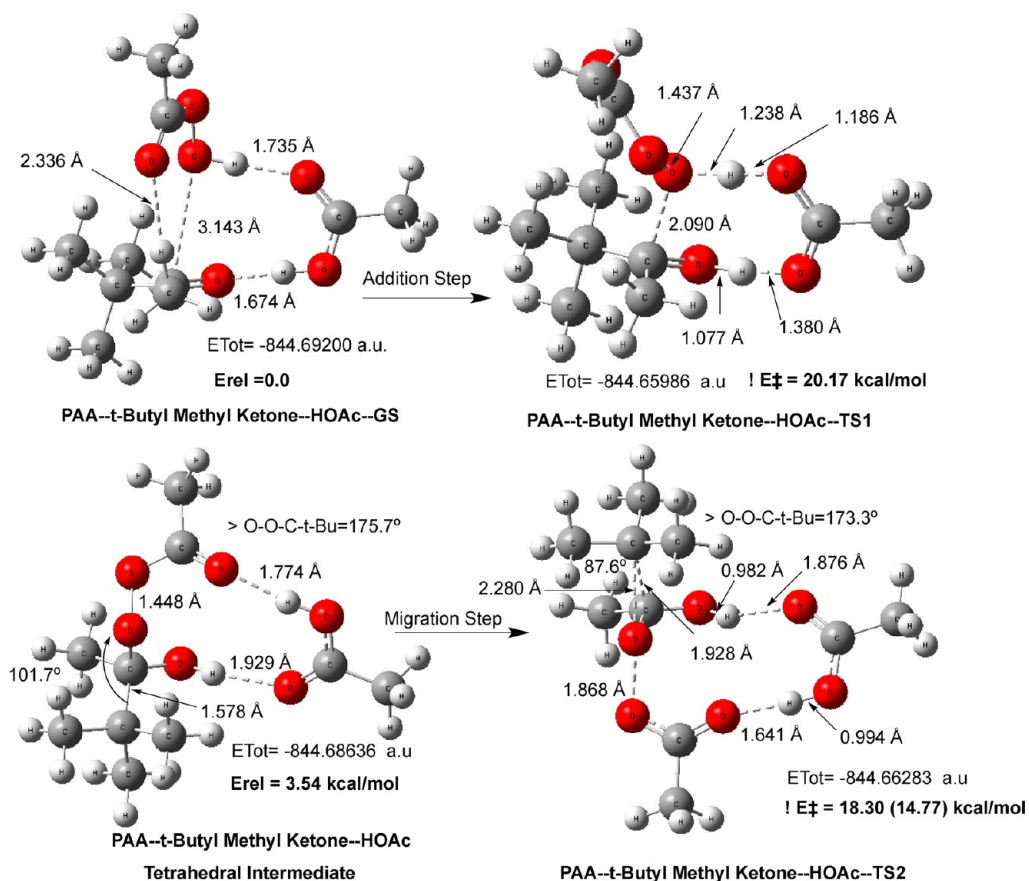


**Figure 6.** Ground-state (GS) complex for peroxyacetic acid and *t*-butyl methyl ketone with acetic acid (HOAc) catalysis and the first transition state (TS1) for the addition of  $\text{CH}_3\text{CO}_3\text{H}$  to form the Criegee tetrahedral intermediate. The transition state (TS2) for the *t*-butyl group migration produces *t*-butyl acetate and acetic acid.

### Scheme 1

	I	II	III
$k$ (1.mole sec.)	$1.47 \times 10^{-5}$	$11.7 \times 10^{-5}$	$1.83 \times 10^{-5}$
Free energy activation kcal/mol ( $\Delta G^\ddagger$ )	24.04 (20.81)	22.81 (19.65)	23.91 (22.22)

concept that the second step in the BV reaction needs little or no catalysis.<sup>2</sup> In this case, the tetrahedral intermediate with the methyl group anti is also slightly lower in energy ( $\Delta E = 0.67$  kcal/mol).

**II. Cyclohexyl Methyl Ketone.** Our next test is to compare the intrinsic barrier for the uncatalyzed addition of peroxyacetic acid to acetophenone (I) versus cyclohexyl methyl ketone (II) to see if the conjugation of an aromatic ring to a  $\text{C}=\text{O}$  affects the rate as previously assumed. We find that the barriers are essentially identical with PAA-cyclohexyl methyl ketone-TS1 (Figure 9) having a barrier that is actually slightly higher ( $\Delta \Delta E^\ddagger = 0.35$  kcal/mol) than the uncatalyzed acetophenone TS1.

When the addition step is HOAc catalyzed, we see a comparable result with the addition of TS (Figure 10) having  $\Delta E^\ddagger = 18.82$  kcal/mol and being 0.79 kcal/mol higher than the

HOAc-catalyzed acetophenone TS1. Caution must be exercised because the orientation of the  $\text{C}=\text{O}$  group can influence the energy of the TS. In this TS (Figure 10), we see the OH of the peroxyacid pointing toward us and the  $\text{CH}_3$  group pointing away. However, we also located a second TS with the opposite orientation, but it was 2.45 kcal/mol higher in energy (not shown). The donor-acceptor nature of the HOAc catalyst is also important because the TS energy ( $\Delta \Delta E^\ddagger = 1.50$  kcal/mol) is lowered if it involves intermolecular H-bonding of the tetrahedral intermediate OH group to the HOAc carbonyl oxygen instead of the intramolecular  $\text{C}=\text{O}$  of the tetrahedral intermediate. We also note that in some cases that using free energies of activation instead of classical activation barriers can lead to slightly different conclusions as pointed out by Alvarez-Idaboy.<sup>11</sup> For example, if we convert the above experimental rate constants (Scheme 1) to free energies of activation they suggest that addition to ketone II should be 7.9 times faster than the phenyl-substituted ketone. Our calculated DFT free energies (Scheme 1) suggest a rate difference of 7.1 (with HOAc catalysis) in favor of the cyclohexyl ketone in excellent agreement with the experimental data. This very close agreement with experimental kinetic data is quite gratifying because we are comparing gas-phase calculations on peroxyacetic acid with experiments that were carried out in chloroform with peroxybenzoic acid.<sup>15a</sup>

The activation energies for the cyclohexyl migration step (TS2) for the uncatalyzed ( $\Delta E^\ddagger = 19.56$  kcal/mol) versus the HOAc-catalyzed rearrangement ( $\Delta E^\ddagger = 19.36$  kcal/mol) are again comparable. However, based upon free energies of



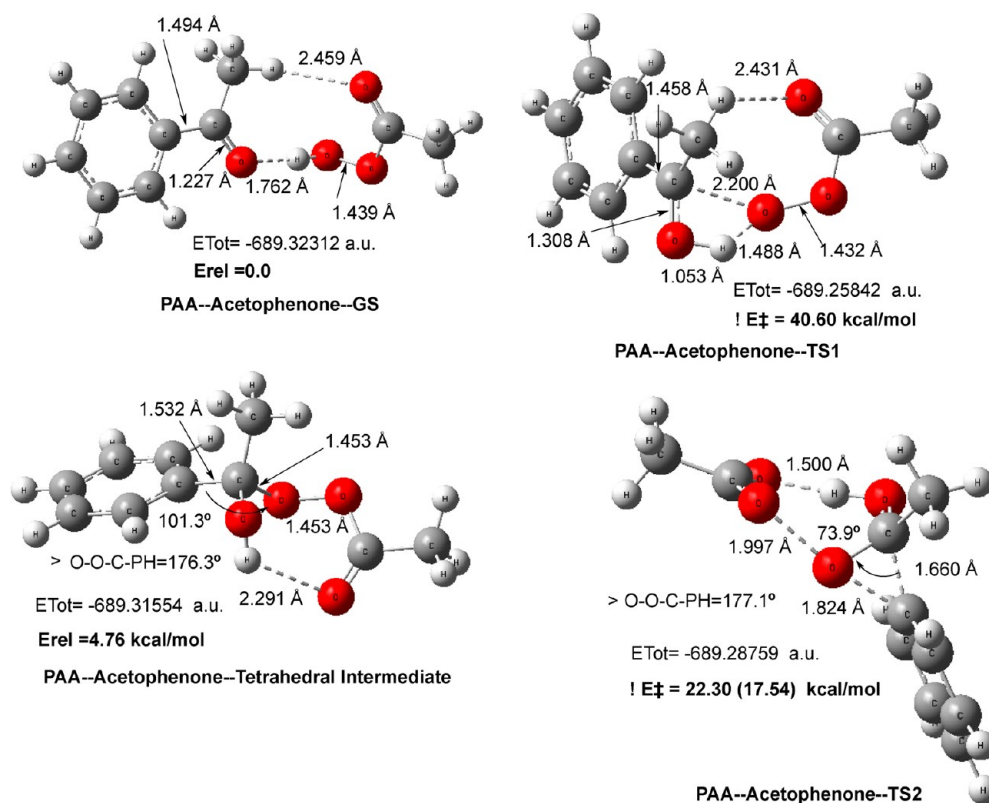


**Figure 7.** Ground-state (GS) complex for peroxyacetic acid and acetophenone and the first transition state (TS1) for the addition of  $\text{CH}_3\text{CO}_3\text{H}$  to form the Criegee tetrahedral intermediate. The transition state (TS2) for the phenyl migration produces phenyl acetate and acetic acid.

activation, the addition step is clearly designated as the rate-limiting step.

**III. Cyclohexyl Phenyl Ketone.** With cyclohexyl phenyl ketone, we have the opportunity to again examine the relative rate of addition to the  $\text{C}=\text{O}$  with an aromatic substituent and also to compare the intramolecular competitive rates of migration of cyclohexyl versus phenyl in the product forming rearrangement step, TS2. The uncatalyzed addition step exhibited a very high barrier as expected ( $\Delta E^\ddagger = 39.72$  kcal/mol), and the migration step had an activation barrier of  $\Delta E^\ddagger = 19.78$  kcal/mol, a value comparable to the other TS2 values reported so far (Figure 11). However, the barrier relative to the total energy of the tetrahedral intermediate is somewhat reduced because this particular Criegee intermediate is 5.52 kcal/mol higher in energy than the GS complex. It is also important to have the dihedral angle of the migrating group approximately antiperiplanar to the breaking  $\text{O}-\text{O}$  moiety. For example, if the angle for the antiperiplanar TS for cyclohexyl migration ( $176.7^\circ$ ) was reduced to  $53^\circ$ , the barrier increased by 15.34 kcal/mol, pointing out the significance of having the migrating group poised in an anti conformation.

The addition step for cyclohexyl phenyl ketone with HOAc catalysis exhibited a relatively high activation barrier ( $\Delta E^\ddagger = 19.04$  kcal/mol) as was expected based upon the kinetic data outlined in Scheme 1. Although the TS is rather congested due to the size of the substituents, the  $\text{O}-\text{C}$  bond representing the addition step ( $r_{\text{C}-\text{O}} = 2.074$  Å) is not noticeably longer (Figure 12). Moreover, the free energy of activation for HOAc-catalyzed addition to cyclohexyl methyl ketone (TS1) was the highest of all three ketones in this series ( $\Delta G^\ddagger = 22.22$  kcal/mol), but most importantly this value was higher than that for

cyclohexyl methyl ketone in good accord with experimental kinetic data discussed above (Scheme 1).

Because this is a ketone with larger substituents, the relative energies of the tetrahedral intermediates are a little higher with the cyclohexyl group being preferred in the anti position ( $\Delta E = 2.78$  kcal/mol) with an  $\text{O}-\text{O}-\text{C}-\text{Ph}$  dihedral angle of  $179.8^\circ$  (Figure 13). In a similar manner, the dihedral angle in TS2 was  $174.7^\circ$ , and the activation barriers for TS2 were also quite low. Cyclohexyl migration was preferred over phenyl migration by 2.77 kcal/mol. Again, we observe the bridging nature for phenyl migration and a relatively short  $\text{C}-\text{C}$  bond distance in the TS (1.690 Å).

The data for the HOAc-catalyzed rearrangement of cyclohexyl versus phenyl migration (Figure 13) exhibit the lowest free energy of activation barriers noted this far with cyclohexyl migration  $\Delta G^\ddagger = 21.48$  kcal/mol and a  $\Delta\Delta G^\ddagger = 2.50$  kcal/mol. This suggests an intramolecular rate ratio of 68 in favor of the cyclohexyl group, while the experimental rate ratio was only 5.<sup>15a</sup>

**e. The Baeyer–Villiger Oxidation with Protonated Acetone.** The above data show the donor–acceptor catalysis of a carboxylic acid functional group in the BV reaction results in a marked reduction in the activation barrier for step one (TS1) irrespective of the ketone involved. When a more active peroxyacid like TFPAA was used in the BV reaction, the addition step had an increased rate, making the migration step rate-determining.<sup>5a</sup> The rather unusual results of the Doering experiment,<sup>4</sup> where sulfuric acid was used as the solvent instead of acetic acid for the BV reaction on benzophenone, showed a rate increase of nearly 400, suggesting a dramatic rate increase for a protonated ketone carbonyl. This prompted us to carry out scouting experiments using peroxyformic acid on

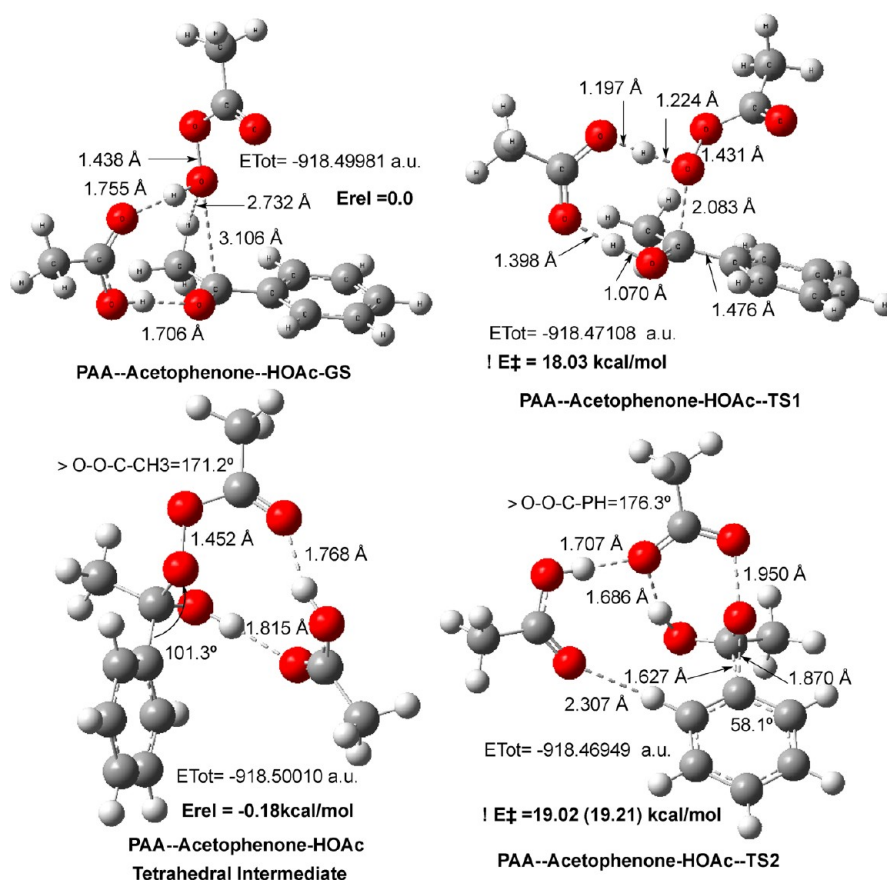


**Figure 8.** Ground-state (GS) complex for peroxyacetic acid and acetophenone and the first transition state (TS1) for the addition of CH<sub>3</sub>CO<sub>3</sub>H with acetic acid (HOAc) catalysis to form the Criegee tetrahedral intermediate. The transition state (TS2) for the phenyl migration produces phenyl acetate and acetic acid.

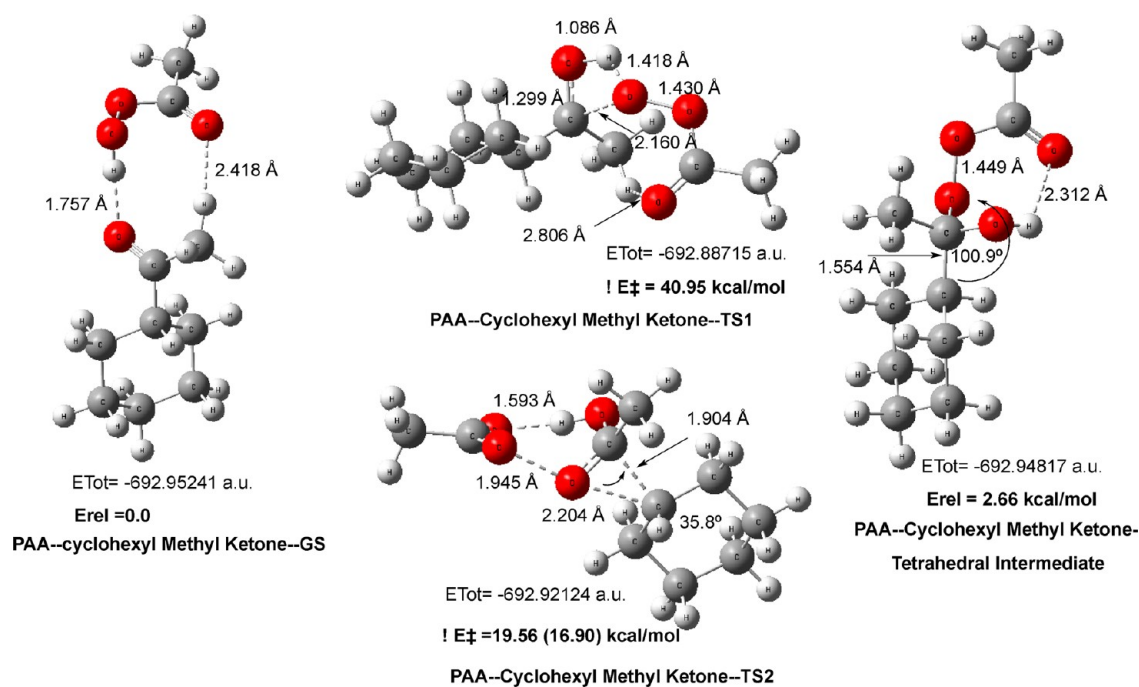


**Figure 9.** Ground-state (GS) complex for peroxyacetic acid and cyclohexyl methyl ketone and the first transition state (TS1) for the addition of CH<sub>3</sub>CO<sub>3</sub>H to form the Criegee tetrahedral intermediate. The transition state (TS2) for the cyclohexyl migration produces cyclohexyl acetate and acetic acid.

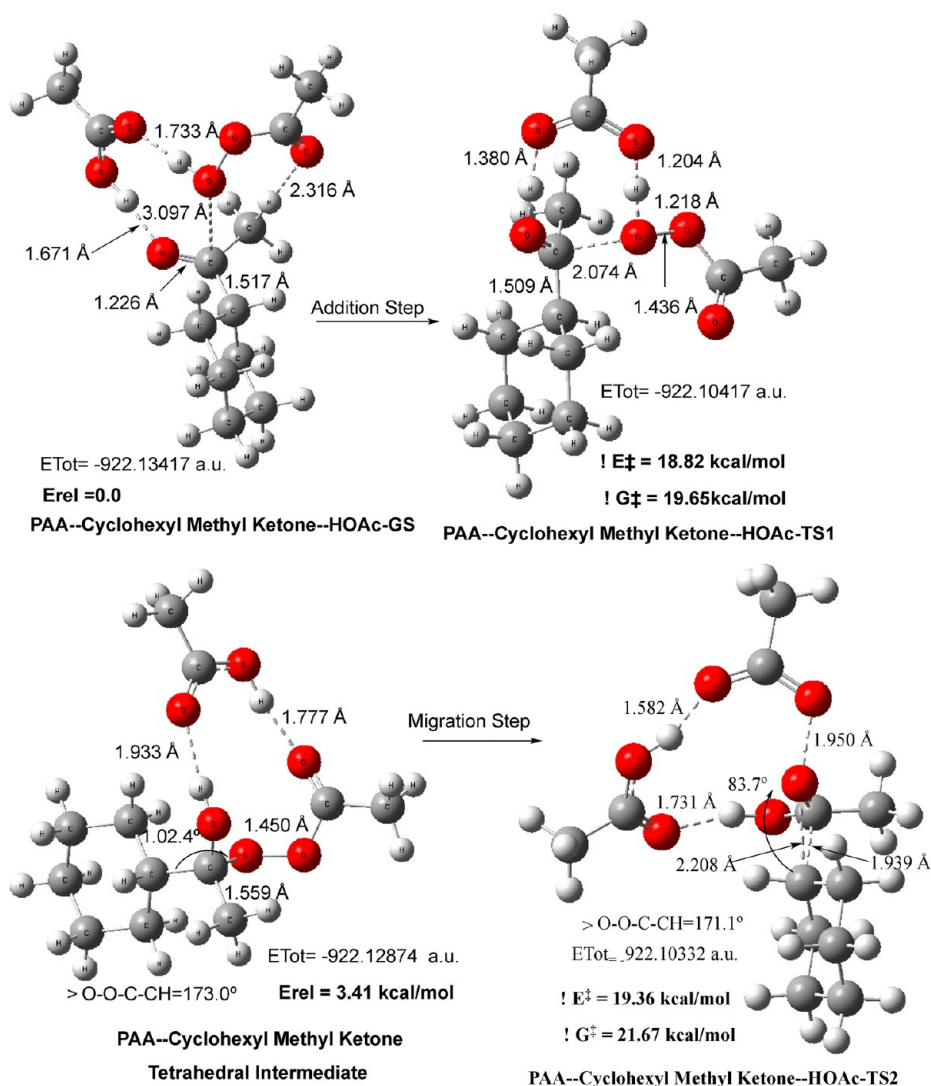


**Figure 10.** Ground-state (GS) complex for peroxyacetic acid and cyclohexyl methyl ketone with acetic acid (HOAc) catalysis and the first transition state (TS1) for the addition of  $\text{CH}_3\text{CO}_2\text{H}$  to form the Criegee tetrahedral intermediate. The transition state (TS2) for cyclohexyl migration produces cyclohexyl acetate and acetic acid.

protonated acetone where we observed a dramatic reduction in both the addition step ( $\Delta E^\ddagger = 11.33$  kcal/mol) and the migration step ( $\Delta E^\ddagger = 8.82$  kcal/mol), and the corresponding structures are given in the Supporting Information (Figure S2).

For the sake of consistency, we carried out the full set of calculations using peroxyacetic acid. The GS complex for protonated acetone and peroxyacetic acid is, as expected, only weakly bound (Figure 14). The TS for addition now has a very different mechanism from both the uncatalyzed and the HOAc-catalyzed addition step. In this case, the proton on the ketone carbonyl oxygen is not involved in any motion in the TS because its role is to activate the  $\text{C}=\text{O}$  for nucleophilic addition of the OOH group. The single imaginary frequency is very high ( $\nu_i = 1154.11$   $\text{cm}^{-1}$ ), and the major contribution to the reaction vector is intramolecular proton transfer from the OOH group to the peroxy acid carbonyl oxygen to render the distal oxygen more nucleophilic. The activation barrier for this first step in the proton-catalyzed peroxyacetic acid addition is the lowest that we have seen thus far ( $\Delta E^\ddagger = 6.50$  kcal/mol). An intrinsic reaction coordinate (IRC) analysis showed that this TS was connected in one direction to its GS precursor and in the other to its tetrahedral intermediate. The migration step

(TS2) is also different from the corresponding rearrangements given above because upon O–O bond cleavage in concert with alkyl group migration a neutral acetic acid molecule is the leaving group with no involvement of the  $\text{C}=\text{OH}^+$  moiety. This atom motion along the reaction path is consistent with a low imaginary frequency ( $\nu_i = 296.71$   $\text{cm}^{-1}$ ) because only O–O and C–C bond breaking was evident upon animation of the reaction vectors. The overall product is the protonated methyl acetate and acetic acid with a  $\Delta E = -68.80$  kcal/mol. The barrier for the migration step is also only  $\Delta E^\ddagger = 4.43$  kcal/mol, and this explains why the Doering experiment<sup>4</sup> in concentrated sulfuric acid proceeded so rapidly. However, it must be noted that such harsh reaction conditions resulted in the formation of secondary products.

## CONCLUSIONS

- (1) The classical activation barriers for the concerted four-center TS for the addition step (TS1) in the BV reaction all exhibit prohibitively high barriers (38–41 kcal/mol) for all of the ketones examined. The BV reaction will not proceed at an acceptable rate in the absence of some

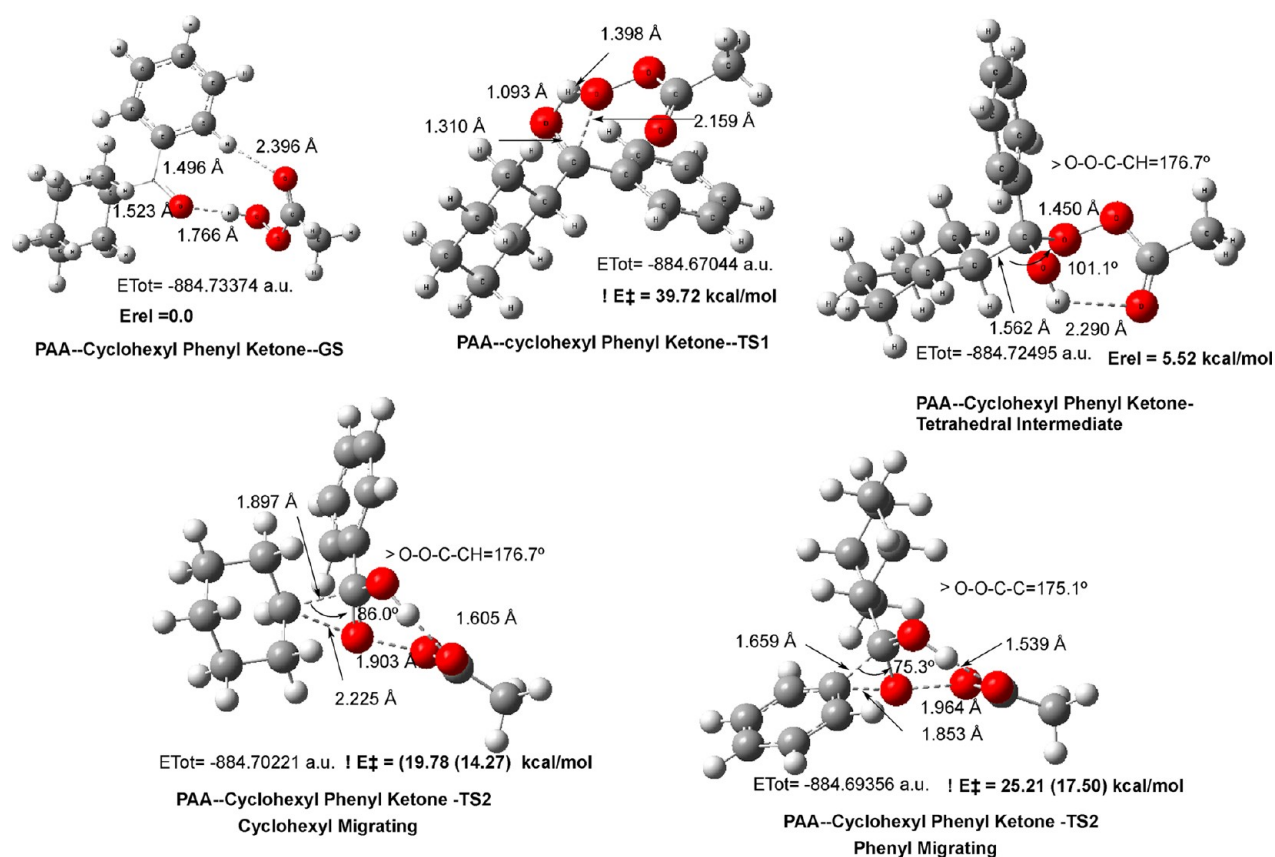


**Figure 11.** Ground-state (GS) complex for peroxyacetic acid and cyclohexyl phenyl ketone and the first transition state (TS1) for the addition of  $\text{CH}_3\text{CO}_3\text{H}$  to form the Criegee tetrahedral intermediate. The transition states (TS2) for cyclohexyl and also phenyl migration produce cyclohexyl acetate and/or phenyl acetate plus acetic acid.

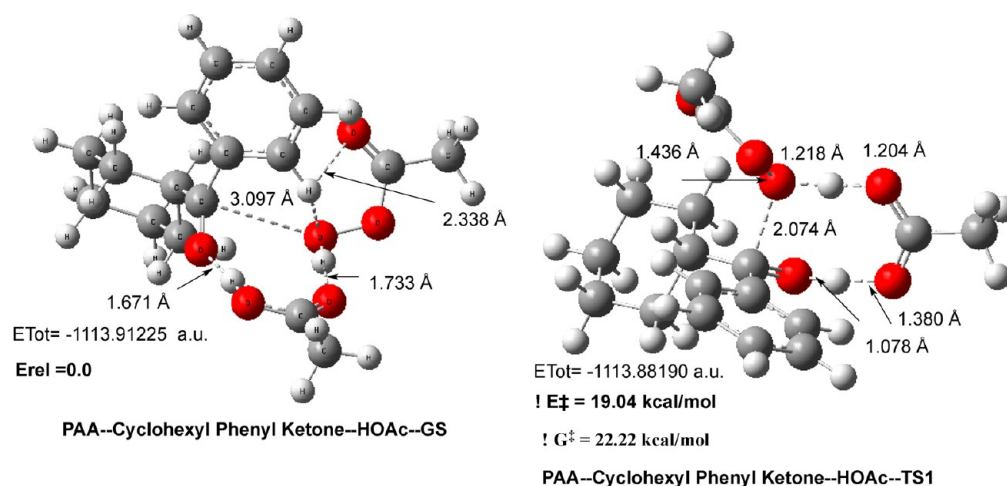


**Figure 12.** Ground-state (GS) complex for peroxyacetic acid and cyclohexyl phenyl ketone with acetic acid (HOAc) catalysis and the first transition state (TS1) for the addition of  $\text{CH}_3\text{CO}_3\text{H}$  to form the Criegee tetrahedral intermediate.

- form of catalysis. In each case, the activation barrier for the second rearrangement step (TS2) was always much lower, leaving no question as to the rate-determining step in the absence of catalysis.
- (2) The COOH functional group can act as a donor–acceptor catalyst in the BV reaction by accepting the proton from the peroxy acid OOH group and transferring its OH proton to the ketone carbonyl, resulting in a marked reduction in activation energy.

- (3) In the absence of relatively strong acids, the first addition step in the BV reaction is rate-determining.
- (4) Protic acids sufficiently strong to protonate the ketone carbonyl oxygen result in marked reductions in activation barriers for both steps in the BV reaction.
- (5) The relative migratory aptitudes for alkyl groups very likely are a consequence of their electron-donating ability.
- (6) The presence of an aryl substituent on the ketone results in a rate reduction of about 7 relative to cyclohexyl

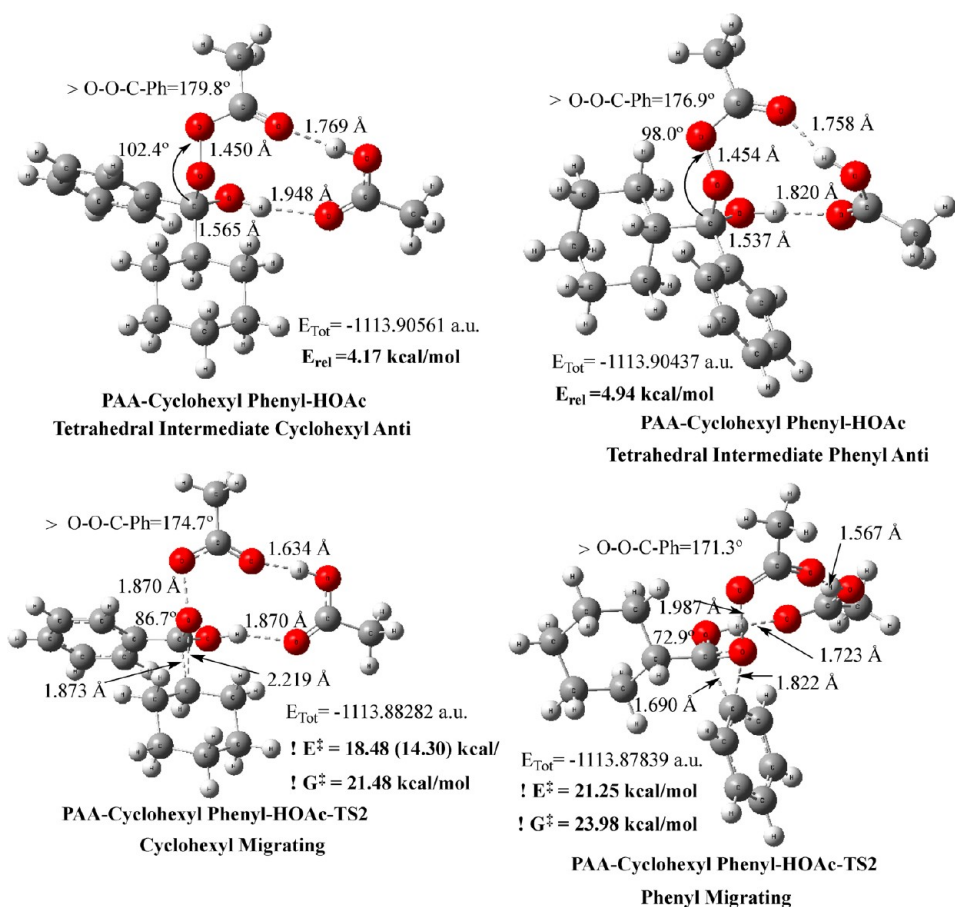


**Figure 13.** The Criegee tetrahedral intermediates derived from peroxyacetic acid addition to cyclohexyl phenyl ketone with HOAc catalysis. The transition states (TS2) for cyclohexyl or phenyl migration produce cyclohexyl and/or phenyl acetate and acetic acid.

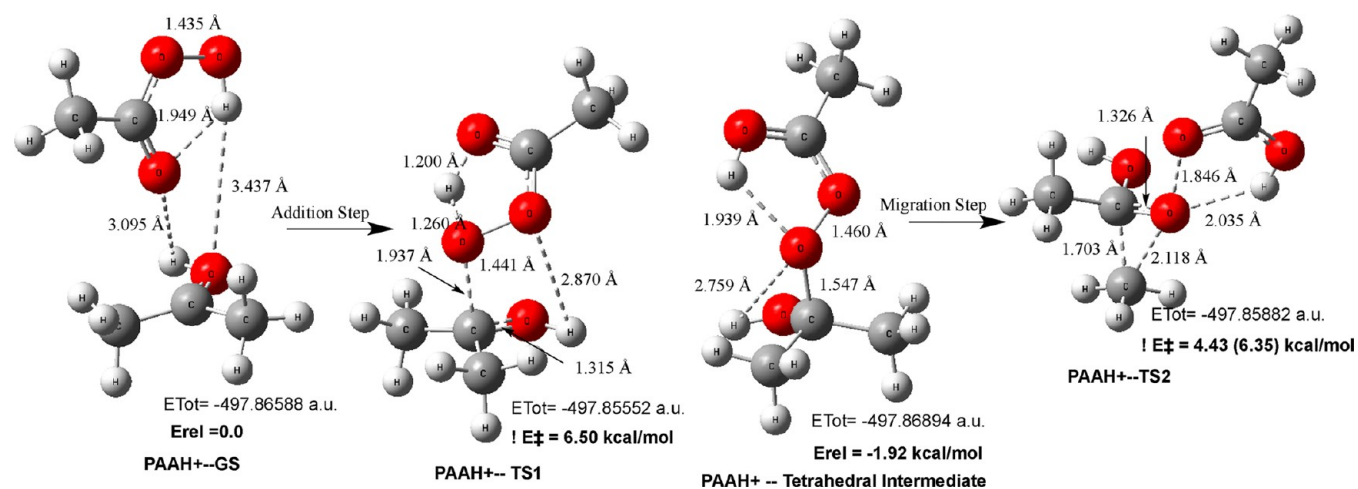


**Figure 14.** Ground-state (GS) complex for peroxyacetic acid and protonated acetone and the first transition state (TS1) for the addition of  $\text{CH}_3\text{CO}_3\text{H}$  to form the Criegee tetrahedral intermediate. The transition state (TS2) for methyl migration produces protonated methyl acetate and acetic acid.

- methyl ketone if the relative rates are based upon free energies of activation. The calculated rate difference for cyclohexyl phenyl ketone was much higher corresponding to a rate difference of about 77, while the experimental rate difference was only 6.
- (7) The migratory preference for *t*-butyl versus methyl in the BV reaction is calculated to be greater than  $10^4$ .

- (8) The migratory preference for cyclohexyl versus phenyl for the methyl ketones was calculated to be about 68 times greater when HOAc catalysis is involved.
- (9) The migration step (TS2) does not require any form of catalysis and exhibits approximately the same activation barriers with and without HOAc catalysis as summarized in Table 1.

Table 1. Calculated Activation Energies  $\Delta E^\ddagger(\Delta G^\ddagger)$  for the Baeyer–Villiger Reaction with Peroxyacetic Acid

transition structure	Figure	ketone	catalyst	barrier <sup>a</sup> $\Delta E^\ddagger$ <sup>b</sup> ( $\Delta G^\ddagger$ ), <sup>c</sup> kcal/mol	freq, cm <sup>-1</sup>
PAA-TS1	3	acetone		37.86	–819.3i
PAA-TS2	3	acetone		22.68	–542.3i
PAA-HOAc-TS1	4	acetone	HOAc	18.83(19.80)	–811.2i
PAA-HOAc-TS2	4	acetone	HOAc	25.25	–488.5i
PAA- <i>t</i> -butyl methyl-TS1	5	<i>t</i> -butyl methyl		40.78(40.2)	–1474.8i
PAA- <i>t</i> -butyl methyl-TS2 <i>t</i> -butyl migrating	5	<i>t</i> -butyl methyl		17.44(20.30)	–234.3i
PAA- <i>t</i> -butyl methyl-TS2 methyl migrating	5	<i>t</i> -butyl methyl		25.09(19.28) <sup>d</sup>	–989.4i
PAA- <i>t</i> -butyl methyl-TS1	6	<i>t</i> -butyl methyl	HOAc	20.17	–834.9i
PAA- <i>t</i> -butyl methyl-TS2	6	<i>t</i> -butyl methyl	HOAc	18.30	–713.8i
PAA-acetophenone-TS1	7	acetophenone (I)		40.60	–437.0i
PAA-acetophenone-TS2	7	acetophenone		22.30	–443.4i
PAA-acetophenone-TS1	8	acetophenone	HOAc	18.03(20.81)	–751.6i
PAA-acetophenone-TS2	8	acetophenone	HOAc	19.02	–346.7i
PAA-cyclohexyl methyl-TS1	9	cyclohexyl methyl (II)		40.95	–704.9i
PAA-cyclohexyl methyl-TS2	9	cyclohexyl methyl		19.56	–351.2i
PAA-cyclohexyl methyl-TS1	10	cyclohexyl methyl	HOAc	18.82(19.65)	–777.3i
PAA-cyclohexyl methyl-TS2	10	cyclohexyl methyl	HOAc	19.36	–347.9i
PAA-cyclohexyl phenyl-TS1	11	cyclohexyl phenyl (III)		39.72	–969.1i
PAA-cyclohexyl phenyl-TS2 (cyclohexyl migrating)	11	cyclohexyl phenyl		19.78	–338.5i
PAA-cyclohexyl phenyl-TS2 (phenyl migrating)	11	cyclohexyl phenyl		25.21(17.50) <sup>e</sup>	–402.4i
PAA-cyclohexyl phenyl-TS1	12	cyclohexyl phenyl	HOAc	19.04(22.22)	–433.1i
PAA-cyclohexyl phenyl-TS2 (cyclohexyl migrating)	13	cyclohexyl phenyl	HOAc	18.48(21.48)	–366.3i
PAA-cyclohexyl phenyl-TS2 (phenyl migrating)	13	cyclohexyl phenyl	HOAc	21.25(23.98)	–397.5i
PAAH+TS1	14	acetone	H+	6.50	–1154.1i
PAAH+TS2	14	acetone	H <sup>+</sup>	4.43	–296.7i

<sup>a</sup>All structures in this table have the B3LYP/6-311+G(d,p) basis set for all atoms. See also individual figures for a more complete description of the structure. <sup>b</sup>The classical barriers ( $\Delta E^\ddagger$ ) are without zero point correction. <sup>c</sup>The activation barrier values in parentheses are free energies of activation ( $\Delta G^\ddagger$ ). <sup>d</sup>Barrier is calculated relative to the lower energy tetrahedral intermediate with the *t*-butyl group antiperiplanar. <sup>e</sup>Barrier is with respect to a tetrahedral intermediate with the phenyl group anti. This conformer is 2.20 kcal/mol higher in energy than the conformer with the cyclohexyl group anti.

- (10) Because the peroxyacids employed in the BV reaction are typically not pure, the presence of the corresponding carboxylic acid at the outset of the reaction was an effective catalyst that increased in concentration during the course of the reaction and was responsible for the autocatalysis often observed. For example, *m*-chloroperbenzoic acid was normally purchased 85% pure.

## COMPUTATIONAL DETAILS

Quantum chemistry calculations were carried out using the Gaussian 09 program<sup>16</sup> system utilizing gradient geometry optimization.<sup>17</sup> In each case, the ground states (GS), transition structures (TS), and overall product tetrahedral intermediates were fully optimized without geometry constraints. Calculations were performed using the B3LYP hybrid density functional<sup>18</sup> with a 6-311+G(d,p) basis set for all atoms. Selected structures were computed using the more recently developed DFT functionals MO6-2X<sup>19a</sup> and MPWB1K<sup>19b</sup> as described above. We have experienced similar erratic behavior with the MPW1K<sup>19c</sup> functional when oxygen atom transfer from flavin hydroperoxides was involved.<sup>14b</sup> While the B3LYP activations were quite close to those derived from QCISD(T) and CCSD(T) calculations, the MPW1K barriers were consistently higher. Each full structure optimization was followed by a complete frequency analysis. The activation barrier for the addition step was calculated relative to the energy of the fully optimized ground-state (GS) complex. In each figure, the barrier for the migration step (TS2) was calculated first relative to its ground-state complex and then relative to its corresponding tetrahedral intermediate, in parentheses, that had the migrating group in the antiperiplanar conformation.

## ASSOCIATED CONTENT

### Supporting Information

Total energies, Cartesian coordinates, and structures. This material is available free of charge via the Internet at <http://pubs.acs.org>.

## AUTHOR INFORMATION

### Corresponding Author

\*E-mail: [rbach@udel.edu](mailto:rbach@udel.edu).

### Notes

The authors declare no competing financial interest.

## ACKNOWLEDGMENTS

We are particularly grateful to GridChem for computational resources ([www.gridchem.org](http://www.gridchem.org)) (see ref 20).

## REFERENCES

- Baeyer, A.; Villiger, V. *Ber* **1899**, *32*, 362S.
- (a) Krow, G. R. *Org. React.* **1993**, *43*, 251. (b) ten Brink, G. T.; Arends, I. W. C. E.; Sheldon, R. A. *Chem. Rev.* **2004**, *104*, 4105.
- (c) Renz, M.; Meunier, B. *Eur. J. Org. Chem.* **1999**, 73.
- (a) Criegee, R. *Justus Liebigs Ann. Chem.* **1948**, 560, 128.
- (b) Goodman, R. M.; Kishi, Y. *J. Am. Chem. Soc.* **1998**, *120*, 9392.
- (4) Doering, W. v. E.; Speers, L. J. *Am. Chem. Soc.* **1950**, *72*, 5515.
- (5) (a) Hawthorne, M. F.; Emmons, W. D. *J. Am. Chem. Soc.* **1958**, *80*, 6398. (b) Mitsuhashi, T. M.; Miyadera, H.; Simamura, O. *J. Chem. Soc., Chem. Commun.* **1970**, 1301.
- (6) (a) Palmer, B. W.; Fry, A. J. *Am. Chem. Soc.* **1970**, *92*, 2580. (b) Ogata, Y.; Sawaki, Y. *J. Org. Chem.* **1969**, *34*, 3985. (c) Ogata, Y.;

Sawaki, Y. *J. Org. Chem.* **1972**, *37*, 2953. (d) Ogata, Y.; Sawaki, Y. *J. Am. Chem. Soc.* **1972**, *94*, 4189.

(7) Singleton, D. A.; Szymanski, M. J. *J. Am. Chem. Soc.* **1999**, *121*, 9455.

(8) Okuno, Y. *Chem.-Eur. J.* **1997**, *3*, 212–218.

(9) Grein, F.; Chen, A. C.; Edwards, D.; Crudden, C. M. *J. Org. Chem.* **2006**, *71*, 861.

(10) Yamabe, S.; Yamazaki, S. *J. Org. Chem.* **2007**, *72*, 3031.

(11) (a) Alvarez-Idaboy, J. R.; Reyes, L.; Cruz, J. *Org. Lett.* **2006**, *8*, 1763. (b) Alvarez-Idaboy, J. R.; Reyes, L. *J. Org. Chem.* **2007**, *72*, 6580.

(c) Alvarez-Idaboy, J. R.; Reyes, L.; Mora-Diez, N. *Org. Biomol. Chem.* **2007**, *5*, 3682. (d) Reyes, L.; Alvarez-Idaboy, J. R.; Mora-Diez, N. *J. Phys. Org. Chem.* **2009**, *22*, 643.

(12) (a) Carlqvist, P.; Eklund, R.; Brinck, T. *J. Org. Chem.* **2001**, *66*, 1193. (b) Itoh, Y.; Yamanaka, M.; Mikami, K. *Org. Lett.* **2003**, *5*, 4803.

(c) Snowden, M.; Bermudez, A.; Kelly, D. R.; Radkiewicz-Poutsma, J. *J. Org. Chem.* **2004**, *69*, 7148. (d) Boronqt, M.; Corma, A.; Renz, M.; Sastre, G.; Viruela, P. M. *Chem.-Eur. J.* **2005**, *11*, 6905. (e) Rivera, D. G.; Pando, O.; Suardiaz, R.; Coll, F. *Steroids* **2007**, *72*, 466.

(13) Woodward, R. B.; Hoffmann, R. *The Conservation of Orbital Symmetry*; Verlag Chemie: Weinheim, 1970.

(14) (a) For a detailed discussion of how the magnitude of the imaginary frequency in the TS for oxygen transfer is related to the nature of the TS, see: Bach, R. D.; Dmitrenko, O. *J. Phys. Chem. B* **2003**, *107*, 12861. (b) Canepa, C.; Bach, R. D.; Dmitrenko, O. *J. Org. Chem.* **2002**, *67*, 8653.

(15) (a) Friess, S. L.; Farnham, N. *J. Am. Chem. Soc.* **1950**, *72*, 5518. (b) Reyes, L.; Castro, M.; Cruz, J.; Rubio, M. *J. Phys. Chem. A* **2005**, *109*, 3383.

(16) (a) Frisch, M. J.; et al. *Gaussian 98*, revision A.7; Gaussian, Inc.: Pittsburgh, PA, 1998. (b) *Gaussian 03*, revision B.05 (SG164-G03RevB.05); Gaussian, Inc.: Pittsburgh, PA, 2003. See the Supporting Information for the full list of authors.

(17) (a) Schlegel, H. B. *J. Comput. Chem.* **1982**, *3*, 214. (b) Schlegel, H. B. *Adv. Chem. Phys.* **1987**, *67*, 249. (c) Schlegel, H. B. In *Modern Electronic Structure Theory*; Yarkony, D. R., Ed.; World Scientific: Singapore, 1995; p 459.

(18) (a) Becke, A. D. *Phys. Rev. A* **1988**, *38*, 3098. (b) Becke, A. D. *J. Chem. Phys.* **1993**, *98*, 5648. (c) Lee, C.; Yang, W.; Parr, R. G. *Phys. Rev. B* **1988**, *37*, 785.

(19) (a) Zhao, Y.; Truhlar, D. G. *Theor. Chem. Acc.* **2008**, *120*, 215.

(b) Zhao, Y.; Truhlar, D. G. *J. Phys. Chem. A* **2004**, *108*, 6908.

(c) Lynch, B. J.; Truhlar, D. G. *J. Phys. Chem. A* **2001**, *105*, 2936.

(20) (a) Dooley, R.; Milfeld, K.; Guiang, C.; Pamidighantam, S.; Allen, G. J. *Grid Comput.* **2006**, *4*, 195. (b) Wilkins-Diehr, N.; Gannon, D.; Oster, S.; Pamidhantam, S. *Teragrid Science Gateways and their Impact on Science, Computer*; IEEE: Los Alamitos, CA, 2008; Vol. 41, pp 32–41.